Zeitschrift: IABSE publications = Mémoires AIPC = IVBH Abhandlungen
Band: 23 (1963)

Artikel: Creep failure of reinforced-concrete columns
Autor: Warner, R.F. / Thürlimann, Bruno
DOI: https://doi.org/10.5169/seals-19410

Creep Failure of Reinforced-Concrete Columns

Influence du fluage sur la rupture des colonnes en béton armé

Einfluß des Betonkriechens auf das Versagen von Stahlbetonsäulen

R. F. WARNER B. THÜRLIMANN
Swiss Federal Institute of Technology, Zurich

1. Introduction

1.1. Creep Failure of Concrete Columns

Although experimental [1] and theoretical [2] studies of creep failure in reinforced concrete columns have been made, no general analytic treatment of the phenomenon is yet available. Difficulties involved in a general analytic approach arise from two main sources:

a) Creep behavior of plain concrete has been investigated for low stresses (Dischinger Creep) but little is known of inelastic behavior in the load range and time span immediately preceding failure.
b) Theoretical treatment of a real cross-section becomes extraordinarily complicated when the neutral axis varies not only with load but also — as a result of creep effects — with time.

In the present paper, a simplified model of plain-concrete behavior is assumed, taking into account the important qualitative findings of RÜSCH [3]. The creep failure of reinforced concrete columns is then investigated. A simplified I section of zero web thickness is considered which simplifies the problem considerably. Numerical evaluation of the equations is nevertheless quite tedious and lends itself to computer programming.

1.2. Approach to Problem

Creep deflection and creep failure in concrete columns occur as a result of the time-dependent deformation and strength properties of plain concrete. The following phenomena are of prime importance:

a) *Variation of concrete strength with duration of load application.* Strength under sustained load is considerably less than under instantly applied failure load [3].

b) *Stress-strain relationship of concrete in bending compression under short-time loading.* This consists of a loading stage to the maximum stress β_0, followed by an unloading stage in which the strain increases to an ultimate value ϵ_u while the stress decreases to some fraction of β_0 [6].

c) *Creep behavior of plain concrete.* For small and intermediate stresses, creep strains follow approximately an exponential variation with time, tending to a limiting value at time infinity. At higher load levels, however, the rate of creep strain is dependent on load magnitude, and the strains tend more to increase uniformly with time until failure occurs.

Because of the change in concrete creep behavior with increasing load, creep of reinforced concrete columns follows a different pattern to that of a steel column at high temperature. Thus, whereas the latter has a finite life for all load values and all eccentricities greater than zero [4], reinforced concrete column behavior can be broken into two distinct phases. This is most conveniently carried out by defining for a given column with a given loading P, an initial critical eccentricity e_{cr} such that for $e \leqq e_{cr}$ the column life is infinite and for $e > e_{cr}$ failure occurs after a finite time interval τ.

Another initial eccentricity e_u may be associated with load P which corresponds to failure of the column under short-time loading ($\tau \to 0$). This type of failure occurs when load P together with the moment M induced by the initial eccentricity e_u plus the elastic column deflection $\overline{w}_0$ cause immediate static failure in the central column section. The static strength of a column *section* has been investigated experimentally and analytically by HOGNESTAD [5] and others. It will be assumed here that the strength properties of a section can be predicted with reasonable accuracy.

In general, $0 < e_{cr} < e_u$, and the creep behavior of a column with eccentric load P can be broken into the following phases:

a) $e = 0$: Strength is independent of creep effects: If the column is slender, the critical buckling load can be determined from the solution of the Eigenvalue problem; if the column is short, the static strength of the section alone governs.

b) $0 < e < e_{cr}$: Creep effects increase the initial deflection and hence the bending moments in the column. This leads to further deflection and creep. However the combined effect of P, e and deflection is not sufficient to cause failure, even after infinite time. The central deflection of the column, $\overline{w}$, will approach a limiting value $\overline{w}_n$.

c) $e = e_{cr}$: Increase in column deflection, hence in bending moment in the center section, is just sufficient to bring the internal stresses to

a state of imminent failure after infinite time ($\tau \to \infty$). Central deflection of the column again approaches a limiting value.

d) $e_{cr} < e < e_u$: Creep induced deflections increase the internal stresses to a state of failure after a finite time interval τ. Column deflection increases until failure takes place.

e) $e = e_u$: Instantaneous ($\tau \to 0$) static failure of the central column section occurs due to load P and moment $(e_u + \overline{w}_0) P$.

Of prime importance in the study of creep behavior is the evaluation of the critical eccentricity e_{cr}. The major portion of this paper deals with the determination of e_{cr} as a function of the load P, the slenderness ratio λ, the cross sectional properties of the column and the parameters defining the strength and deformation characteristics of plain concrete.

2. Strength and Deformation Characteristics of Plain Concrete

2.1. Concrete Strength as a Function of Time of Loading

The experimental work of RÜSCH has shown that the strength of axially loaded concrete specimens is dependent on the rate at which the loading is applied and on the time τ over which the loading is maintained. This phenomenon is indicated qualitatively in Fig. 1 where β_τ represents the concrete

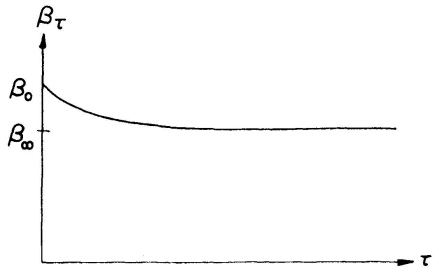

Fig. 1.

strength corresponding to sustained loading time τ. Values given by RÜSCH indicate that concrete strength under long sustained ($\tau \to \infty$) loading, β_∞, can vary between seventy-five and eighty-five percent of the concrete strength under short-time ($\tau \to 0$) loading, β_0:

$$K_\infty = \frac{\beta_\infty}{\beta_0} = 0.75\,; \quad \text{fast initial loading rate (one hour)},$$

$$= 0.85\,; \quad \text{very gradually applied load (time of load application} \approx \tau).$$

Since the decrease in strength with increasing τ is approximately exponential, the relation can be expressed approximately as

$$\beta_\tau = \beta_\infty + (\beta_0 - \beta_\infty)\, e^{-\alpha_1 \tau} \tag{2.1}$$

or non-dimensionally as $K_\tau = K_\infty + (1 - K_\infty)\, e^{-\alpha_1 \tau}$, (2.2)

where $K_\tau = \dfrac{\beta_\tau}{\beta_0}$

and α_1 is a parameter defining the appropriate time units. Since α_1 becomes important only in the case of finite life problems, it will not be evaluated here.

Eq. (2.1) applies only to the case of sustained loading of constant magnitude. No test data has yet been published for the situation in which the concrete stress σ varies in the range $\beta_\infty < \sigma < \beta_0$. A simple linear damage assumption might however be made, similar to the Palmgren-Miner hypothesis for fatigue failure. With the failure time interval corresponding to σ_i denoted as τ_i and the actual loading time of σ_i as $\Delta\tau_i$, the linear damage assumption leads to the failure criterion

$$\sum \frac{\Delta\tau_i}{\tau_i} = 1. \tag{2.3}$$

Such an expression is also required only in the treatment of finite-life problems.

2.2. *Concrete Stress-strain Relation, $\tau \to 0$*

The actual stress-strain relation for concrete under short-time loading can be approximated [6] quite well by a cubic parabola for the loading curve and a second order parabola for the unloading curve, as shown in Fig. 2a. In the present work, however, the relation will be simplified to the three straight lines shown in Fig. 2b. The value ϵ' corresponding to the stress $\sigma = \beta_\infty$ must of course be chosen to give best fit to the experimental curve.

2.3. *Creep Behavior*

For relatively small stresses, creep behavior is represented with reasonable accuracy by the Eqs. [7]

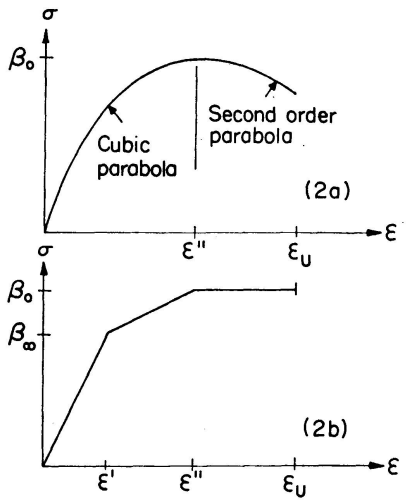

Fig. 2.

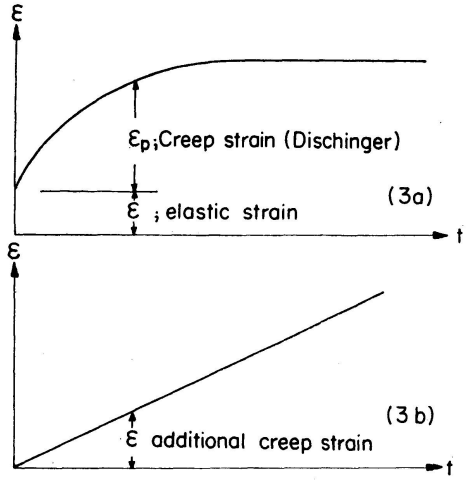

Fig. 3.

$$\dot{\epsilon} = \frac{\sigma}{E_c}\dot{\Phi} + \frac{\dot{\sigma}}{E_c}, \tag{2.4}$$

$$\Phi = \Phi_n (1 - e^{-\alpha_2 t}). \tag{2.5}$$

The parameter α_2 and the value of the creep function at time infinity, Φ_n, must be obtained from tests. Although these equations were originally derived for creep behavior in the lower load levels, their range of applicability will be assumed here to extend up to the stress β_∞. This extrapolation should not lead to serious error provided the experimental value of Φ_n is obtained as a mean from tests conducted over the full range $0 < \sigma < \beta_\infty$.

For high stresses, however, creep strains no longer tend to a limiting value but increase with time until failure. This behavior can be treated by introducing a second creep term in addition to the DISCHINGER function as shown in Fig. 3. This term is expressed as

$$\epsilon_i = t\,\alpha_3 \tan\varphi.$$

Assuming a linear relation between the extreme values

$$\sigma = \beta_\infty; \qquad \varphi = 0,$$

and

$$\sigma = \beta_0; \qquad \varphi = \frac{\pi}{2},$$

we have

$$\epsilon_i = t\,\alpha_3 \tan\frac{\sigma - \beta_\infty}{\beta_0 - \beta_\infty}\frac{\pi}{2}. \tag{2.6}$$

Thus for constant stress $\sigma > \beta_\infty$

$$\epsilon = \epsilon_{el}\{1 + \Phi_n (1 - e^{-\alpha_2 t})\} + t\,\alpha_3 \tan\left(\frac{\sigma - \beta_\infty}{\beta_0 - \beta_\infty}\frac{\pi}{2}\right) \tag{2.7}$$

and for variable stress $\beta_\infty < \sigma < \beta_0$,

$$\dot{\epsilon} = \frac{\dot{\sigma}}{E_c} + \frac{\sigma}{E_c}\dot{\Phi} + \alpha_3 \tan\left(\frac{\sigma - \beta_\infty}{\beta_0 - \beta_\infty}\frac{\pi}{2}\right). \tag{2.8}$$

Again, Eqs. (2.7) and (2.8) are required only in the study of finite life problems.

3. Static Strength of Section

3.1. Instantaneous Loading, $\tau \to 0$

The strength of a reinforced concrete section subjected to moment M and thrust P can be conveniently represented by an interaction diagram [5] similar to Fig. 4. For the simplified section of Fig. 6a which will be treated in the present study, this diagram consists of two intersecting straight lines, one representing compression failure, the other tension failure, as shown in Fig. 5.

Compression failure under short-time loading occurs when the steel stress in the compression flange is at yield, $\sigma_{sl} = \sigma_y$, and the concrete stress in the same flange is stressed to β_0, $\sigma_l = \beta_0$. Equilibrium of forces leads to the equation

$$P = 2\left\{\beta_0 A_c + \sigma_y A_s - \frac{M^0}{h}\right\}. \tag{3.1}$$

In the extreme case of zero moment,

$$P_u^0 = 2\{\beta_0 A_c + \sigma_y A_s\}. \tag{3.2}$$

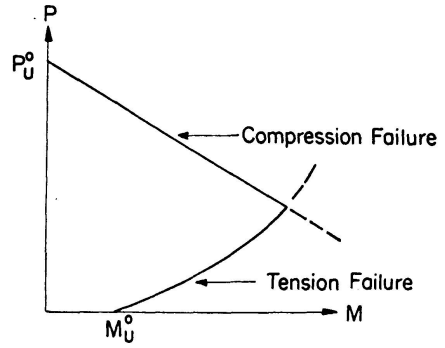

Fig. 4.

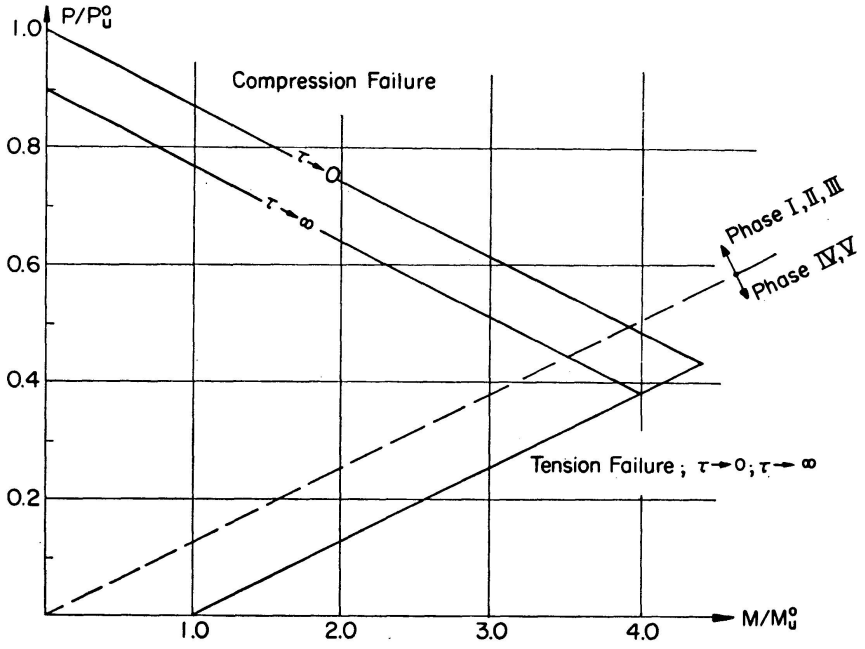

Fig. 5.

For tension failure, we may write immediately

$$M^0 = h\,\sigma_y A_s + \tfrac{1}{2} P h \tag{3.3}$$

with the extreme value for zero axial force

$$M_u^0 = h\,\sigma_y A_s. \tag{3.4}$$

Eqs. (3.1) and (3.3) may be non-dimensionalized to yield the more convenient forms:

Compression Failure, $\tau \to 0$:

$$\left(\frac{P^0}{P_u^0}\right) = 1 - \frac{1}{\zeta_1}\left(\frac{M^0}{M_u^0}\right). \tag{3.5}$$

Tension Failure, $\tau \to 0$:

$$\left(\frac{M^0}{M_u^0}\right) = 1 + \zeta_1 \left(\frac{P}{P_u^0}\right), \tag{3.6}$$

in which

$$\zeta_1 = 1 + \frac{\beta_0}{\mu \sigma_y} \tag{3.7}$$

and μ is the proportion of steel area in one flange, A_s/A_c.

3.2. Sustained Loading $\tau \to \infty$

When the loading is sustained over the time interval $\tau \to \infty$ the failure condition in the compression flange becomes $\sigma_l = \beta_\infty$ and $\sigma_{sl} = \sigma_y$. Tension failure is however unchanged. The equations are thus:

Compression Failure, $\tau \to \infty$

$$\left(\frac{P}{P_u^0}\right) = \zeta_2 \left\{1 - \frac{1}{\zeta_1}\left(\frac{M^\infty}{M_u^0}\right)\right\}. \tag{3.8}$$

Tension Failure, $\tau \to \infty$

$$\left(\frac{M^\infty}{M_u^0}\right) = 1 + \zeta_1 \left(\frac{P}{P_u^0}\right), \tag{3.6a}$$

in which

$$\zeta_2 = \frac{\beta_\infty + \mu \sigma_y}{\beta_0 + \mu \sigma_y}. \tag{3.9}$$

4. Creep Behavior of Concrete Column

4.1. Introduction

Equations will now be derived to describe the creep behavior of a pin-ended concrete column with a sustained load P applied at an initial eccentricity e. The column cross section is shown in Fig. 6a, the loading arrangement in Fig. 6c. The prime purpose of the analysis is to determine the critical

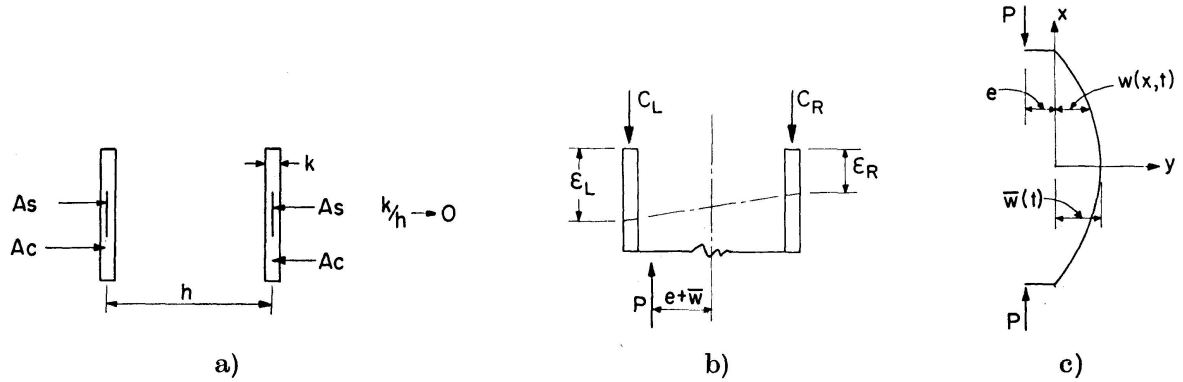

Fig. 6.

eccentricity e_{cr} which induces a state of failure after an infinite time interval $\tau \to \infty$. Since the concrete stresses will not exceed β_∞, concrete creep behavior will be defined by Eqs. (2.4) and (2.5).

The internal actions M and P in the central cross section may be superimposed on the interaction diagram defining the strength of the section as shown in Fig. 7a. The line $0Z$ represents the application of axial force P at

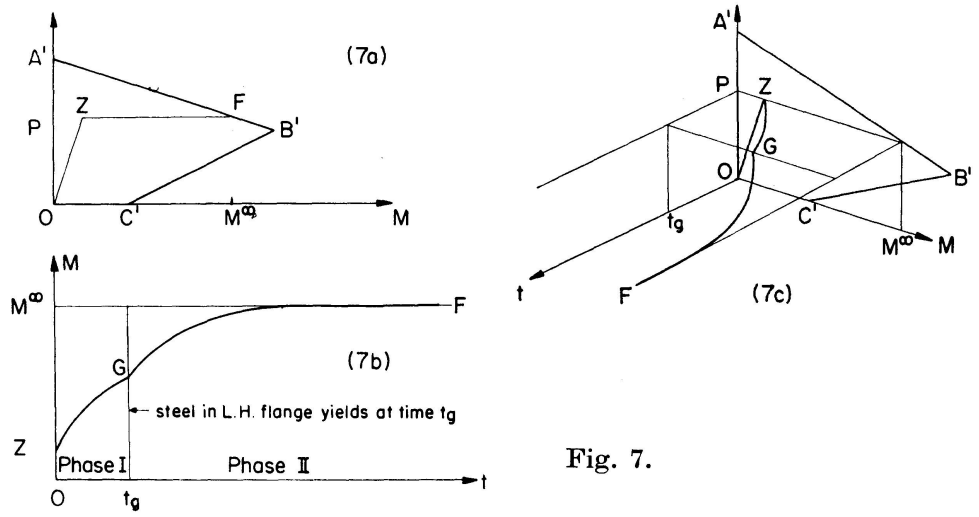

Fig. 7.

eccentricity e. The horizontal line ZF with P constant represents the increase in lateral deflection. The initial eccentricity is equal to e_{cr} if the point F representing conditions at infinite time lies on the failure envelope $A'B'C'$.

Considering the state of stress in the flanges of the member, we see that a number of different possibilities can arise for the loading arrangement of Fig. 6c. The possible states of stress in the central column cross section are summarized in Table 1.

The equilibrium conditions and hence the creep analysis are different for each of the phases shown. Furthermore, the creep effect in a given column will usually begin in one phase but pass into a second and, possibly, a third as the process continues. This is illustrated qualitatively in Figs. 7b and 7c, where

Table 1. Stress Phases in Central Section of Column
(Compression positive)

Phase	Left Hand Flange		Right Hand Flange	
	Strain	Steel Stress.	Strain	Steel Stress
I	$+\epsilon_l$	$\sigma_{sl} < \sigma_y$	$+\epsilon_r$	$\sigma_{sr} < \sigma_y$
II	$+\epsilon_l$	$\sigma_{sl} = \sigma_y$	$+\epsilon_r$	$\sigma_{sr} < \sigma_y$
III	$+\epsilon_l$	$\sigma_{sl} = \sigma_y$	$+\epsilon_r$	$\sigma_{sr} = \sigma_y$
IV	$+\epsilon_l$	$\sigma_{sl} < \sigma_y$	$-\epsilon_r$	$\sigma_{sr} > -\sigma_y$
V	$+\epsilon_l$	$\sigma_{sl} = \sigma_y$	$-\epsilon_r$	$\sigma_{sr} > -\sigma_y$

the changes indicated in Fig. 7a are shown in terms of the time parameter. The point G represents a change of phase occurring at time t_g.

Equilibrium of internal forces in the center section of the column, for all phases and at any time t, is expressed by the equations

$$C_l + C_r = P, \qquad \frac{h}{2}(C_l - C_r) = (e + \bar{w})\,P,$$

in which $\bar{w}$ is the lateral deflection of the center section. Furthermore, P is held constant in the present analysis, so that

$$\dot{C}_l + \dot{C}_r = \dot{P} = 0, \qquad \frac{h}{2}(\dot{C}_l - \dot{C}_r) = P\dot{\bar{w}}.$$

Introducing non-dimensional terms for initial eccentricity and central deflection,

$$\kappa = e/h, \tag{4.1}$$

$$\delta = \bar{w}/h, \tag{4.2}$$

we may re-write the equilibrium equations as

$$C_l = P(0.5 + \kappa + \delta), \tag{4.3}$$

$$C_r = P(0.5 - \kappa - \delta), \tag{4.4}$$

$$\dot{C}_l = P\dot{\delta}, \tag{4.5}$$

$$\dot{C}_r = -P\dot{\delta}. \tag{4.6}$$

The force C_l consists of a concrete force and a steel force, i.e.

$$C_l = \sigma_l A_c + \sigma_{sl} A_s.$$

The concrete stress in the left hand flange for all phases is therefore

$$\sigma_l = \frac{P}{A_c}\{0.5 + \kappa + \delta\} - \mu\,\sigma_{sl} \tag{4.7}$$

and its derivative is

$$\dot{\sigma}_l = \frac{P}{A_c}\dot{\delta} - \mu\,\dot{\sigma}_{sl}. \tag{4.8}$$

For phases I, II, and III, the concrete stress in the right hand flange is

$$\sigma_r = \frac{P}{A_c}\{0.5 - \kappa - \delta\} - \mu\,\sigma_{sr} \tag{4.9}$$

and

$$\dot{\sigma}_r = -\frac{P}{A_c}\dot{\delta} - \mu\,\dot{\sigma}_{sr}. \tag{4.10}$$

In phases IV and V the right hand flange is in tension, the concrete stress is zero,

$$\sigma_r = 0$$

the steel stress is
$$\sigma_{sr} = \frac{P}{A_s}(0.5-\kappa-\delta) \tag{4.11}$$

and
$$\dot{\sigma}_{sr} = -\frac{P}{A_s}\dot{\delta}. \tag{4.12}$$

Considering now the deformation of the column, and using the cosine approximation for the column curve, we write

$$w(x,t) = \overline{w}(t)\cos\frac{\pi x}{l}.$$

The curvature at the mid section is therefore

$$\frac{1}{\rho} = -\frac{\pi^2}{l^2}\overline{w}(t). \tag{4.13}$$

The internal strains are assumed to be positive when compressive, as in Fig. 6 b, so that we also have

$$-\frac{1}{\rho} = \frac{\epsilon_l-\epsilon_r}{h}. \tag{4.14}$$

Combination of (4.13) and (4.14) yields

$$(\epsilon_l-\epsilon_r) = \pi^2\frac{h^2}{l^2}\delta.$$

Introduction of the slenderness-ratio λ, which for the section under consideration is equal to $2l/h$, results in

$$\delta = \frac{\lambda^2}{4\pi^2}(\epsilon_l-\epsilon_r) \tag{4.15}$$

and
$$\dot{\delta} = \frac{\lambda^2}{4\pi^2}(\dot{\epsilon}_l-\dot{\epsilon}_r). \tag{4.16}$$

It will be convenient now to evaluate the initial column deflection at time zero, δ_0. This value will depend upon the starting phase, which, in practice, will almost certainly be either I or IV, depending upon the magnitude of P.

For phase I, equilibrium of internal forces, together with the elastic stress-strain relations, yield

$$\epsilon_{l0} = \frac{P(0.5+\kappa+\delta_0)}{A_c E_c(1+n\mu)} \tag{4.17}$$

and
$$\epsilon_{r0} = \frac{P(0.5-\kappa-\delta_0)}{A_c E_c(1+n\mu)}. \tag{4.18}$$

Substitution of these values into (4.15) gives

$$\delta_0\left(4\pi^2\frac{A_c E_c(1+n\mu)}{P\lambda^2}-2\right) = 2\kappa.$$

With the definitions
$$\eta_c = \frac{4\pi^2 A_c E_c}{\lambda^2 P}, \tag{4.19}$$

$$\eta_s = \frac{4\pi^2 A_s E_s}{\lambda^2 P} \tag{4.20}$$

the expression for δ_0 in phase I becomes

$$\delta_0 = \frac{2\kappa}{\eta_c + \eta_s - 2}. \tag{4.21}$$

The initial concrete strain in the left hand flange is then found to be

$$\epsilon_{l0} = \frac{P}{A_c E_c (1+n\mu)} \left(0.5 + \frac{\eta_c + \eta_s}{\eta_c + \eta_s - 2} \kappa\right). \tag{4.22}$$

A similar treatment for phase IV provides the equations

$$\delta_0 = \frac{(1+2n\mu)\kappa - 0.5}{n\mu(1+n\mu)\eta_c - (1+2n\mu)} \tag{4.23}$$

and

$$\epsilon_{l0} = \frac{P}{As\,Es} \{(\eta_s - 1)\delta_0 + 0.5 - \kappa\}. \tag{4.24}$$

The creep behavior in each of the five possible phases will now be treated in turn.

4.2. Phase I

Since in phase I the entire section is in compression, creep effects will take place in both flanges. Eq. (2.4) is therefore applied to each flange:

$$\dot{\epsilon}_l = \frac{\sigma_l}{E_c}\dot{\Phi} + \frac{\dot{\sigma}_l}{E_c}, \tag{2.4a}$$

$$\dot{\epsilon}_r = \frac{\sigma_r}{E_c}\dot{\Phi} + \frac{\dot{\sigma}_r}{E_c}. \tag{2.4b}$$

The above equations are substituted into (4.16) to give

$$\frac{4\pi^2\dot{\delta}}{\lambda^2} = \frac{\sigma_l - \sigma_r}{E_c}\dot{\Phi} + \frac{\dot{\sigma}_l - \dot{\sigma}_r}{E_c} \tag{4.25}$$

and the terms $(\sigma_l - \sigma_r)$ and $(\dot{\sigma}_l - \dot{\sigma}_r)$ are rewritten using Eqs. (4.7), (4.8), (4.9) and (4.10) together with the additional information that $\sigma_{sl} = E_s \epsilon_l$ and $\sigma_{sr} = E_s \epsilon_r$ to yield

$$\frac{4\pi^2\dot{\delta}}{\lambda^2} = \left\{\frac{P}{A_c E_c}(2\kappa + 2\delta) - \frac{4\pi^2}{\lambda^2} n\mu\delta\right\}\dot{\Phi} + \left\{\frac{2P}{A_c E_c} - \frac{4\pi^2}{\lambda^2} n\mu\right\}\dot{\delta},$$

which is equivalent to

$$\left\{4\pi^2 \frac{A_c E_c + A_s E_s}{\lambda^2 P} - 2\right\}\frac{\partial\delta}{\partial\Phi} = \left\{2 - \frac{4\pi^2 A_s E_s}{\lambda^2 P}\right\}\delta + 2\kappa$$

or, with the notation of (4.19) and (4.20),

$$\frac{\eta_c + \eta_s - 2}{2 - \eta_s}\frac{\partial\delta}{\partial\Phi} = \delta + \frac{2\kappa}{2 - \eta_s}. \tag{4.26}$$

The initial condition for Eq. (4.26) is given at time $t = 0$ as

$$\Phi = 0; \quad \delta = \delta_0.$$

The solution to (4.26) may now be expressed in the form

$$\frac{2\kappa+(2-\eta_s)\delta}{2\kappa+(2-\eta_s)\delta_0}=\exp\left[\frac{2-\eta_s}{\eta_c+\eta_s-2}\Phi\right] \tag{4.27a}$$

provided

$$\eta_s \neq 2. \tag{4.28a}$$

For the case when (4.28a) is not fulfilled, i.e.

$$\eta_s = 2 \tag{4.28b}$$

the δ term drops out of (4.26) and integration of the equation yields

$$\delta=\delta_0+\frac{2\kappa}{\eta_c}\Phi \tag{4.27b}$$

Eqs. (4.27a) and (4.27b) allow δ and hence the moment in the mid-length section of the column to be determined at any time t in phase *I*.

In order later to couple phase I with phase II, it will be necessary to obtain a solution also for ϵ_l. Substituting for σ_l and $\dot{\sigma}_l$ in (2.4a) we first obtain

$$\dot{\epsilon}_l=\left\{\frac{P}{A_c E_c}(0.5+\kappa+\delta)-n\mu\epsilon_l\right\}\dot{\Phi}+\frac{P}{A_c E_c}\dot{\delta}-n\mu\dot{\epsilon}_l$$

or

$$\frac{\partial\epsilon_l}{\partial\Phi}+\frac{n\mu}{1+n\mu}\epsilon_l=\frac{P}{A_c E_c+A_s E_s}\left(0.5+\kappa+\delta+\frac{\partial\delta}{\partial\Phi}\right). \tag{4.29}$$

From Eq. (4.27a) we then obtain

$$\delta+\frac{\partial\delta}{\partial\Phi}=\kappa\left\{\frac{2}{2-\eta_s}-\frac{2\eta_c^2}{(\eta_s-2)(\eta_c+\eta_s-2)^2}\exp\left[\frac{2-\eta_s}{\eta_c+\eta_s-2}\Phi\right]\right\}.$$

Substitution of the above expression into (4.29) yields the first order linear differential equation

$$\frac{\partial\epsilon_l}{\partial\Phi}+\frac{n\mu}{1+n\mu}\epsilon_l=$$
$$\frac{P}{A_c E_c+A_s E_s}\left\{\frac{1}{2}+\kappa\left[\frac{\eta_s}{\eta_s-2}-\frac{2\eta_c^2}{(\eta_s-2)(\eta_c+\eta_s-2)}\exp\left(\frac{2-\eta_s}{\eta_c+\eta_s-2}\Phi\right)\right]\right\}, \tag{4.30}$$

which may be solved using the initial condition

$$\Phi=0;\quad \epsilon_l=\epsilon_{l0}$$

to give

$$\epsilon_l=\epsilon_{l0}\exp\left(-\frac{n\mu}{1+n\mu}\Phi\right)$$
$$+\frac{P}{A_s E_s}\left(\frac{1}{2}-\frac{\eta_s\kappa}{2-\eta_s}\right)\left[1-\exp\left(-\frac{n\mu}{1+n\mu}\Phi\right)\right] \tag{4.31a}$$
$$+\frac{P}{A_c E_c}\frac{\eta_c^2\kappa}{(2-\eta_s)(\eta_c+\eta_s-2)}\left[\exp\left(\frac{2-\eta_s}{\eta_c+\eta_s-2}\Phi\right)-\exp\left(-\frac{n\mu}{1+n\mu}\Phi\right)\right].$$

The above equation does not hold when $\eta_s = 2$. For this condition, substitution of (4.27b) and its derivative into (4.29) yields the differential equation

$$\frac{\partial \epsilon_l}{\partial \Phi} + \frac{n\mu}{1+n\mu}\epsilon_l = \frac{P}{A_c E_c + A_s E_s}\left[0.5+\kappa+\delta_0+\frac{2\kappa}{\eta_c}(1+\Phi)\right]$$

the solution of which is

$$\epsilon_l = \epsilon_{l0} + \frac{P}{A_s E_s}\frac{2\kappa}{\eta_c}\Phi \tag{4.31b}$$

for condition (4.28b).

The value of Φ at which the steel reinforcement in the left hand flange reaches yield can be evaluated from Eq. (4.31) by replacing ϵ_l by ϵ_y and making a trial and error solution for Φ.

The range of application of the above equations is determined by the requirements that the force in the right hand flange is compressive and that all steel stresses are elastic; hence by the relations

$$M \leqq \frac{Ph}{2}, \qquad 0 < \sigma_{sl} < +\sigma_y, \qquad 0 < \sigma_{sr} < +\sigma_y.$$

4.3. Phase II

In phase II the entire section is again in compression and Eqs. (2.4a), (2.4b), (4.7), (4.8), (4.9) and (4.10) may again be substituted into (4.16), this time with $\sigma_{sl} = \sigma_y$ and $\sigma_{sr} = E_s \epsilon_r$, to give

$$\frac{4\pi^2\dot{\delta}}{\lambda^2} = \frac{P}{A_c E_c}\left[\frac{1}{2}+\kappa+\delta-\frac{0.5-\kappa-\delta}{1+n\mu}\right]\dot{\Phi} - \left[\mu\frac{\sigma_y}{E_c} - \frac{n\mu}{1+n\mu}\epsilon_r\right]\dot{\Phi} + \frac{P}{A_c E_c}\frac{2+n\mu}{1+n\mu}\dot{\delta}.$$

Changing the derivative from t to Φ and solving for ϵ_r we obtain

$$\begin{aligned}\epsilon_r = {} & \left[\frac{4\pi^2(1+n\mu)}{\lambda^2 n\mu} - \frac{P}{A_c E_c}\frac{2+n\mu}{n\mu}\right]\frac{\partial\delta}{\partial\Phi} + \frac{1+n\mu}{n\mu}\mu\frac{\sigma_y}{E_c} \\ & - \frac{P}{A_s E_s}[(1+n\mu)(0.5+\kappa+\delta) - (0.5-\kappa-\delta)]\end{aligned} \tag{4.32}$$

and hence

$$\frac{\partial \epsilon_r}{\partial \Phi} = \left[\frac{4\pi^2(1+n\mu)}{\lambda^2 n\mu} - \frac{P}{A_c E_c}\frac{2+n\mu}{n\mu}\right]\frac{\partial^2\delta}{\partial\Phi^2} - \frac{P}{A_s E_s}(2+n\mu)\frac{\partial\delta}{\partial\Phi}. \tag{4.33}$$

From (2.4a), however,

$$\frac{\partial \epsilon_l}{\partial \Phi} = \frac{P}{A_c E_c}(0.5+\kappa+\delta) - \mu\frac{\sigma_y}{E_c} + \frac{P}{A_c E_c}\frac{\partial\delta}{\partial\Phi}. \tag{4.34}$$

Differentiation of (4.15) with respect to Φ gives

$$\frac{\partial \epsilon_l}{\partial \Phi} - \frac{\partial \epsilon_r}{\partial \Phi} = \frac{4\pi^2}{\lambda^2}\frac{\partial\delta}{\partial\Phi}$$

and substitution of (4.33) and (4.34) yields the second order equation

$$\frac{\partial^2 \delta}{\partial \Phi^2} + \frac{\eta_c \eta_s - 2\eta_c - 2\eta_s}{\eta_c^2 + \eta_c \eta_s - 2\eta_c - \eta_s} \frac{\partial \delta}{\partial \Phi} - \frac{\eta_s}{\eta_c^2 + \eta_c \eta_s - 2\eta_c - \eta_s} \delta = \frac{\eta_s}{\eta_c^2 + \eta_c \eta_s - 2\eta_c - \eta_s} \left(0.5 + \kappa - \frac{A_s \sigma_y}{P}\right). \tag{4.35}$$

The first initial condition for the above equation is of the form

$$\Phi = \Phi_g; \qquad \delta = \delta_g.$$

Usually Φ_g will refer to the instant when the steel in the left hand flange reaches yield, i.e. when $\epsilon_l = \epsilon_y$. The value of Φ_g will therefore be obtained as the value of phase I.

The second initial condition is obtained from Eq. (4.32) by solving for the first derivative of δ:

$$\frac{\partial \delta}{\partial \Phi} = \frac{1}{\eta_c + \eta_s - (2 + n\mu)} \left[\frac{A_s E_s}{P} \epsilon_r + (\kappa + \delta)(2 + n\mu) + \frac{n\mu}{2} - (1 + n\mu) \frac{A_s \sigma_y}{P}\right]. \tag{4.36}$$

The initial value $\left(\frac{\partial \delta}{\partial \Phi}\right)_g$ is then obtained by substituting the initial value $(\epsilon_r)_g$ which can be determined from the end condition of phase I:

$$\left(\frac{\partial \delta}{\partial \Phi}\right)_g = \frac{1}{\eta_c + \eta_s - (2 + n\mu)} \left[\frac{A_s E_s}{P} (\epsilon_r)_g + (\kappa + \delta_g)(2 + n\mu) + \frac{n\mu}{2} - (1 + n\mu) \frac{A_s \sigma_y}{P}\right]. \tag{4.37}$$

Eq. (4.35) is of the form

$$\frac{\partial^2 \delta}{\partial \Phi^2} + a_1 \frac{\partial \delta}{\partial \Phi} + a_2 \delta = a_3$$

its solution is thus

$$\delta = C_1 e^{r_1 \Phi} + C_2 e^{r_2 \Phi} + \left[0.5 + \kappa - \frac{A_s \sigma_y}{P}\right], \tag{4.38}$$

in which C_1 and C_2 are integration constants, and r_1 and r_2 are the two solutions of the quadratic equation

$$r^2 + a_1 r + a_2 = 0.$$

The constants C_1 and C_2 are evaluated using the initital conditions;

$$\begin{bmatrix} e^{r_1 \Phi_g} & e^{r_2 \Phi_g} \\ r_1 e^{r_1 \Phi_g} & r_2 e^{r_2 \Phi_g} \end{bmatrix} \begin{bmatrix} C_1 \\ C_2 \end{bmatrix} = \begin{bmatrix} \left(\delta_g - 0.5 - \kappa + \frac{A_s \sigma_y}{P}\right) \\ \left(\frac{\partial \delta}{\partial \Phi}\right)_g \end{bmatrix}.$$

The region of phase II is defined by the relations

$$M \leqq \tfrac{1}{2} P h, \qquad \sigma_{sl} = +\sigma_y, \qquad 0 < \sigma_{sr} < +\sigma_y.$$

In order to determine the limit $\sigma_{sr}=\sigma_y$, the expression for δ, i.e. Eq. (4.38), together with its derivative, may be substituted into (4.32) to give

$$(\epsilon_r)_{\bar{y}} = \epsilon_y = [\eta_c+\eta_s-(2+n\mu)]\frac{P}{A_s E_s}\left(\frac{\partial\delta}{\partial\Phi}\right)_{\bar{y}}+(1+n\mu)\epsilon_y - \frac{P}{A_s E_s}\left[(2+n\mu)(\kappa+\delta_{\bar{y}})+\frac{n\mu}{2}\right]. \tag{4.39}$$

This expression allows the value $\Phi_{\bar{y}}$ to be determined at which a phase change from II to III occurs.

4.4. *Phase III*

A treatment of phase III similar to that of phase I, but with the values $\sigma_{sl}=\sigma_{sr}=\sigma_y$, leads to the first order equation

$$\left\{\frac{4\pi^2}{\lambda^2}-\frac{2P}{A_c E_c}\right\}\frac{\partial\delta}{\partial\Phi} = \frac{2P}{A_c E_c}(\delta+\kappa)$$

or

$$\left\{\frac{1}{2}\eta_c-1\right\}\frac{\partial\delta}{\partial\Phi} = \delta+\kappa. \tag{4.40}$$

With the initial condition

$$\Phi = \Phi_y; \qquad \delta = \delta_y$$

obtained as the end condition of phase II, the solution of (4.40) may be written as

$$\frac{\kappa+\delta}{\kappa+\delta_y} = \exp\left\{\frac{2}{\eta_c-2}(\Phi-\Phi_y)\right\}. \tag{4.41}$$

The range of application of this equation is governed by the conditions

$$M = Ph/2, \qquad \sigma_{sl} = +\sigma_y, \qquad \sigma_{sr} = +\sigma_y.$$

4.5. *Phase IV*

Since in phase IV the right hand flange is in tension, $\sigma_r=0$ and the creep effect takes place only in the left flange. From (4.11)

$$\epsilon_r = \frac{P}{A_s E_s}(0.5-\kappa-\delta)$$

and

$$\dot{\epsilon}_r = -\frac{P}{A_s E_s}\dot{\delta}. \tag{4.42}$$

The derivative $\dot{\epsilon}_l$ may be evaluated from Eqs. (4.16) and (4.42) as

$$\dot{\epsilon}_l = \left[\frac{4\pi^2}{\lambda^2}-\frac{P}{A_s E_s}\right]\dot{\delta}. \tag{4.43}$$

The concrete stress in the left hand flange is obtained from Eq. (4.7),

$$\sigma_l = \frac{P}{A_c}[0.5+\kappa+\delta]-\mu E_s \epsilon_l,$$

so that

$$\dot{\sigma}_l = \frac{P}{A_c}\dot{\delta}-\mu E_s \dot{\epsilon}_l.$$

Substituting for $\dot{\epsilon}_l$, σ_l and $\dot{\sigma}_l$ into the creep function (2.4a) we obtain

$$\left[\frac{4\pi^2}{\lambda^2}-\frac{P}{A_s E_s}\right]\dot{\delta} = \frac{P}{A_c E_c}(2\kappa+2\delta)\dot{\Phi}-\frac{4\pi^2}{\lambda^2}\delta\mu n\dot{\Phi} + \left[\frac{2P}{A_c E_c}-\frac{4\pi^2}{\lambda^2}\mu n\right]\dot{\delta},$$

which simplifies to

$$\left(\eta_c+\eta_s-\frac{1+2n\mu}{n\mu}\right)\frac{\partial\delta}{\partial\Phi} = (2-\eta_s)\delta+2\kappa. \tag{4.44}$$

With the initial condition

$$\Phi = \Phi_g; \qquad \delta = \delta_g$$

the solution of (4.43) is

$$\frac{2\kappa+(2-\eta_s)\delta}{2\kappa+(2-\eta_s)\delta_g} = \exp\left[\frac{2-\eta_s}{\eta_c+\eta_s-\frac{1+2n\mu}{n\mu}}(\Phi-\Phi_g)\right]. \tag{4.45a}$$

Eq. (4.45a) does not hold when $\eta_s = 2$.

In this particular case, direct integration of (4.44) gives

$$(\delta-\delta_g) = 2n\mu\kappa(\Phi-\Phi_g). \tag{4.45b}$$

The region of phase IV is defined as

$$M \geqq Ph/2, \qquad 0<\sigma_{sl}<+\sigma_y, \qquad -\sigma_y<\sigma_{sr}<0.$$

4.6. Phase V

The analysis for phase V is most easily obtained by eliminating $\dot{\epsilon}_l$ from the two basic Eqs. (2.4a) and (4.16) to give

$$\frac{4\pi^2\dot{\delta}}{\lambda^2} = \frac{\sigma_l}{E_c}\dot{\Phi}+\frac{\dot{\sigma}_l}{E_c}-\dot{\epsilon}_r.$$

Substitution of the quantities

$$\dot{\epsilon}_r = -\frac{P}{A_s E_s}\dot{\delta}$$

and

$$\sigma_l = \frac{P}{A_c}(0.5+\kappa+\delta)-\mu\sigma_y$$

results in the equation

$$\left(\eta_c-\frac{1+n\mu}{n\mu}\right)\frac{\partial\delta}{\partial\Phi} = \delta+\left(0.5+\kappa-\frac{A_s\sigma_y}{P}\right). \tag{4.46}$$

With initial condition $\Phi = \Phi_g$; $\delta = \delta_g$

we thus obtain

$$\frac{\delta + 0.5 + \kappa - \frac{A_s \sigma_y}{P}}{\delta_g + 0.5 + \kappa - \frac{A_s \sigma_y}{P}} = \exp\left[\frac{\Phi - \Phi_g}{\eta_c - \frac{1+n\mu}{n\mu}}\right]. \tag{4.47}$$

The region of phase V is

$$M \geqq Ph/2, \qquad \sigma_{sl} = +\sigma_y, \qquad -\sigma_y < \sigma_{sr} < 0.$$

4.7. Critical Eccentricity

The creep behavior of a column with the load applied at the critical eccentricity e_{cr} will usually involve two — and possibly three — of the phases treated above. Although the condition separating phases I, II and III from IV and V is simple, $\kappa + \delta = \frac{1}{2}$, it is not known before the calculations are made at which stage the two further conditions, $\epsilon_l = \epsilon_y$, and $\epsilon_r = \epsilon_y$, will occur. Thus it will not always be known in advance which phases will be encounted. Because also of the large number of possible phase combinations and the relative complexity of stating the coupling conditions in general terms, solution for e_{cr} in closed form is hardly feasible.

A trial and error method is more suitable, in which an initial value for κ (i.e., initial eccentricity) is first chosen, the initial phase is determined from the conditions of Table 1, and the initial creep behavior is treated using the appropriate equations. Either phase I or phase II will govern initially. The value Φ_g will then be determined for which either

$$\delta + \kappa = \tfrac{1}{2}$$

or

$$\epsilon_l = \epsilon_y,$$

i.e., for which a change of phase occurs. Further creep behavior is then determined in the new phase, either up to the value Φ_g at a second change of phase or to the end value Φ_n. The final deflection $h\,\delta_n$ which corresponds to $\Phi = \Phi_n$, i.e. $t = \infty$, is thus obtained.

However, the total eccentricity e'_∞ which will cause static failure in the column *section* after time infinity can be obtained for load P from the $M - P$ interaction diagram of Fig. 5, as

$$e'_\infty = \frac{M}{P}.$$

The correct initial value for κ has therefore been chosen when the following equality is fulfilled:

$$\kappa + \delta_n = \frac{e'_\infty}{h},$$

i.e. when

$$e = e_{cr} = e'_\infty - \overline{w}_n.$$

All of the equations required for this trial and error procedure are contained above. The application of the analysis will be demonstrated in the following section with a numerical example which will provide actual data on the effect on column strength of creep deflections.

5. Numerical Example

The following computations are made for a simplified I section with the following properties:

$$\begin{aligned} A_c &= 300 \text{ in}^2 \\ A_s &= 3 \text{ in}^2 \ (\mu = 0.01) \\ h &= 30 \text{ in} \\ \beta_0 &= 3400 \text{ psi} \\ \beta_\infty &= 3000 \text{ psi} \ (K_\infty = 0.883) \\ \sigma_y &= 50{,}000 \text{ psi} \\ E_s &= 30 \cdot 10^6 \text{ psi} \\ E_c &= 3 \cdot 10^6 \text{ psi} \\ \Phi_n &= 3 \end{aligned}$$

The Equations of Section 3 yield the following static strength values:

$$\begin{aligned} P_u^0 &= 2.34 \cdot 10^6 \text{ lb}, \\ P_u^\infty &= 2.10 \cdot 10^6 \text{ lb}, \\ \frac{P_u^\infty}{P_u^0} &= 0.897, \\ M_u^\infty &= M_u^0 = 4.5 \cdot 10^6 \text{ in lb}. \end{aligned}$$

For balanced (simultaneous) tension and compression failure under short-time loading, $\tau \to 0$,

$$\left(\frac{P}{P_u^0}\right) = 0.436; \qquad \left(\frac{M}{M_u^0}\right) = 4.400,$$

and for long sustained loading, $\tau \to \infty$,

$$\left(\frac{P}{P_u^0}\right) = 0.384; \qquad \left(\frac{M}{M_u^0}\right) = 4.000.$$

The above values have been used to obtain the interaction diagram of Fig. 5 and the line $\lambda = 0$ in Fig. 8.

Creep calculations have been made for four different slenderness ratios; $\lambda = 20$, 40, 60 and 80. A trial and error procedure was used in which an initial value of κ was chosen, and the calculations made to determine the final value of the deflection term δ_n. The calculations were repeated until the κ_{cr} value

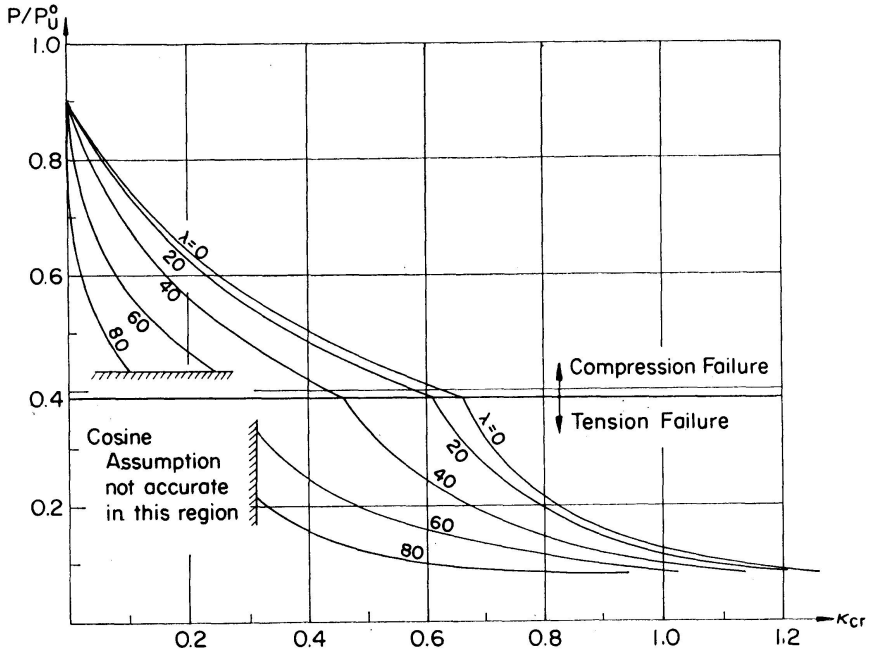

Fig. 8.

Table 2. Numerical Example

No.	λ	$\frac{P^\alpha}{P_u^0}$	$\frac{M^\alpha}{M_u^0}$	$\delta_n + \kappa_{cr}$	η_c *)	κ_{cr}	**)	δ_0	$\frac{\delta_n}{\delta_0}$
1	20	0.086	1.667	1.250	444.0	1.222	IV	0.020	1.40
2	40	0.086	1.667	1.250	111.0	1.136	IV	0.078	1.46
3	60	0.086	1.667	1.250	49.3	0.990	IV	0.163	1.59
4	80	0.086	1.667	1.250	27.8	0.794	IV	0.244	1.87
5	20	0.158	2.220	0.906	240.0	0.873	IV	0.022	1.50
6	40	0.158	2.220	0.906	60.0	0.768	IV	0.078	1.77
7	60	0.158	2.220	0.906	26.7	0.598	IV	0.125	2.46
8	80	0.158	2.220	0.906	15.0	0.388	I	0.027	19.16
9	20	0.315	3.455	0.703	120.0	0.654	IV	0.024	2.04
10	40	0.315	3.455	0.703	30.0	0.516	IV	0.057	3.28
11	60	0.315	3.455	0.703	13.4	0.320	I	0.025	15.30
12	80	0.315	3.455	0.703	7.5	—	—	—	—
13	20	0.450	3.500	0.500	84.6	0.465	I	0.005	7.00
14	40	0.450	3.500	0.500	21.2	0.350	I	0.016	9.37
15	60	0.450	3.500	0.500	9.4	0.220	I	0.027	10.02
16	80	0.450	3.500	0.500	5.3	0.083	I	0.022	19.00
17	20	0.630	2.085	0.212	60.2	0.190	I	0.003	7.33
18	40	0.630	2.085	0.212	15.1	0.134	I	0.009	8.66
19	60	0.630	2.085	0.212	6.7	0.060	I	0.011	13.83
20	80	0.630	2.085	0.212	3.8	0.011	I	0.005	40.02
21	60	0.211	2.660	0.810	20.0	0.450	IV	0.040	9.00
22	60	0.735	1.270	0.112	5.7	0.023	I	0.005	17.80

*) $\eta_s = 0.10\ \eta_c$ in present example.
**) Initial Phase.

was obtained which gave a final $(\kappa_{cr}+\delta_n)$ value, and hence moment, equal to that indicated by the interaction diagram for $\tau \to \infty$.

The results of the calculations are summarized in Table 2 and have been used to plot Figs. 8 and 9. A sample calculation, No. 15, is given in detail in the Appendix.

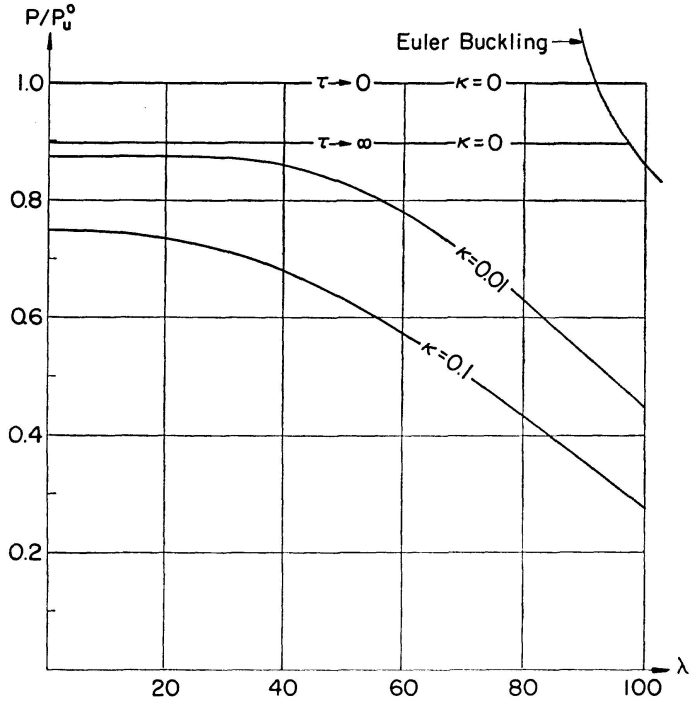

Fig. 9.

In Fig. 8 the value $\kappa_{cr}=e_{cr}/h$ is plotted against load for the four λ-values. In the higher load range, $P/P_u^0 \geqq 0.5$, it is seen that the critical eccentricity e_{cr} is less than $0.05\,h$ for a slenderness ratio of 80 or more. Since "accidental" eccentricities of this order must always be anticipated in practice, creep failure after a finite time interval should be reckoned with in such columns.

For slenderness ratios of 60 the eccentricity must be reduced to nearly half of the section failure eccentricity, e'_∞, in order to prevent creep failure. Only for very short columns, $\lambda < 20$, is the effect negligible.

The portions of the lines $\lambda = 60$ and 80 not plotted in Fig. 8 represent a region in which the analysis does not hold. In this region the accuracy of the cosine approximation to the column curve falls off and, over a small range of values, cannot be made at all. The reason is that the state of stress here passes through phase IV, for which a minimum value of η_s must be stated. Eq. (4.43) may be rearranged to the form

$$\dot{\epsilon}_l = (\eta_s - 1)\frac{P}{A_s E_s}\dot{\delta},$$

which indicates that η_s must be greater than unity in order that $\dot{\epsilon}_l$ and $\dot{\delta}$ be both positive. This means that for η_s-values less than unity, the left hand

flange would be required to unload as the column deflection increases. This physically impossible situation derives from the inapplicability of Eq. (4.43), hence from the inapplicability here of the cosine assumption. A more accurate column curve would have to be used to obtain accurate results in this region.

In Fig. 9 the load required to produce failure for $\tau \to \infty$ is plotted against slenderness ratio for two initial eccentricities of $e = 0.01\,h$ and $0.1\,h$. For purposes of comparison a portion of the Euler buckling curve is also shown in the figure. It lies high above the two failure lines, and, in fact, does not even apply to the present range of interest, since $P_E/P_u^0 < 1.0$ for $\lambda < 80$.

6. Summary and Conclusion

The present study has been limited to the case of a column with an idealized section consisting of thin flanges and a web of zero thickness. Choice of this section simplifies the analysis enormously and allows an overall view of the creep effect to be obtained. The behavior of an actual column of rectangular section with steel in both faces should parallel, at least qualitatively, that of this ideal section.

In the present approach, creep failure is treated as a second order deflection problem with a time-dependent static failure criterion of the central section subjected to combined bending and thrust.

The critical initial eccentricity e_{cr}, which is used to divide creep behavior into the cases of finite life ($e > e_{cr}$), and no-failure ($e \leqq e_{cr}$), is of prime significance. Although the design of columns for specified finite life might, with further research, be feasible, errors in predicted "life" are likely to be very large, owing to the form of the creep function and to the variations to be expected in the concrete creep properties. Finite life analysis may therefore prove to be similar to the analysis of fatigue life, requiring statistical treatment. Furthermore, due to the exponential form of the creep function, the difference between the infinite life load P_u^∞ and, say, the fifty-year life load P_u^{50} should not be great and it would seem advisable, at least until further, more detailed studies are made, to limit column eccentricities (or, alternatively, column loadings) to ensure infinite life, i.e. $e \leqq e_{cr}$.

The creep behavior of a reinforced-concrete column has been seen to depend on the state of stress in the steel, and, depending upon that state of stress, passes through a number of different phases as the column deflection increases. Creep deflections can to some extent be controlled by an increase in the steel area A_s. The effect of A_s is represented in the equations of Section 4 by the term $\eta_s = \frac{4\pi^2}{\lambda^2}\frac{A_s E_s}{P}$. Far more effective, however, is a decrease in the slenderness ratio λ which occurs squared in both the steel term η_s and the concrete term $\eta_c = \frac{4\pi^2}{\lambda^2}\frac{A_c E_c}{P}$. The prime parameters affecting the value of e_{cr} have been found to be η_c, η_s and the limiting creep value Φ_n.

The results of the numerical example provide interesting information on creep failure. In the higher load range $(P/P_u^0) \geqq 0.5$, the critical eccentricity for slender columns ($\lambda \geqq 80$) becomes exceedingly small, $e_{cr} < 0.05\,h$. Since "accidental" eccentricities of this order must always be reckoned with, the calculations would indicate that creep failure in such columns is extremely likely.

In the lower load ranges and for less slender columns, the considerable reduction in eccentricity required by time dependent lateral deflection is shown in Fig. 8. For columns with slenderness ratios in the range $40 < \lambda < 60$ the reduction in moment can be more than 50 percent when the load P is in the order of $0.4\,P_u^0$. Thus, a column designed for a sustained loading producing a thrust $P = 0.4\,P_u^0$ and a maximum moment $M = 0.5\,M_u(P_u^0)$ may well have a finite life.

The calculations have also indicated limitations to the equations derived in Section 4. In particular, the use of the cosine function for the column curve has already limited the applicability of the equations of phases IV and V for slenderness ratios $\lambda \geqq 60$. An improvement may however be made without essentially altering the approach developed here. Use of a numerical integration procedure to eliminate the cosine curve approximation should not present any inherent difficulty, but will complicate the calculations and will almost certainly necessitate the use of a computer for numerical evaluation.

A second major assumption limiting the applicability of this work is of course the use of a simplified I section. A closer approximation to an actual column section may be obtained by dividing the section not into two, but three or more layers spaced uniformly over the width h, as shown in Fig. 10. With the total concrete area $A = \sum A_i$ equal to the actual section area, and the steel spaced as in the actual section, the approximation should be adequate. In such an analysis the two simultaneous differential Eqs. (2.4a) and (2.4b)

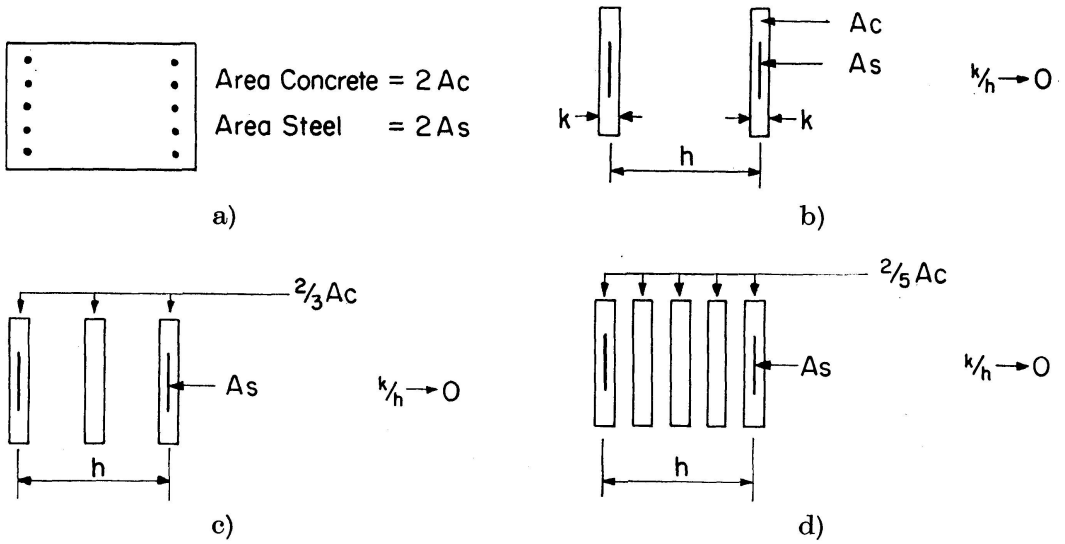

Fig. 10.

would be replaced by a series of simultaneous equations equal in number to the number of layers chosen.

In the present study, concrete creep behavior has been linearized by applying Eq. (2.4) throughout the region $0 < \sigma < \beta^{\infty}$. A more accurate analysis can be made by choosing two (or more) regions, for example $0 < \sigma < 0.5\beta^{\infty}$, $0.5\beta^{\infty} < \sigma < \beta^{\infty}$, and using a different linear creep function in each region. Such a refinement is hardly warrented until more experimental data is obtained on concrete behavior in the higher stress ranges and on strength characteristics under sustained loadings.

Acknowledgement

The work described in this paper was conducted in the Institut für Baustatik und Massivbau, E.T.H., Zürich, with the financial assistance of the Committee for Code Revision, Swiss Engineers and Architects Society (Schweizerischer Ingenieur- und Architekten-Verein).

Nomenclature

A_c = concrete area in one flange.

A_s = steel area in one flange.

C_l = total force in left hand flange, center section.

C_r = total force in right hand flange, center section.

$K_\tau = \frac{\beta_\tau}{\beta_0}$.

$K_\infty = \frac{\beta_\infty}{\beta_0}$.

M = moment in center section.

M^0 = moment causing instantaneous ($\tau \to 0$) failure in section subjected to axial thrust P.

M^∞ = moment causing failure after infinite time ($\tau \to \infty$) in section subjected to axial thrust P.

M_u^0 = flexural capacity of section under short-time loading ($P = 0$; $\tau \to 0$).

M_u^∞ = flexural capacity of section under sustained loading ($P = 0$; $\tau \to \infty$).

P = applied load.

P_u^0 = ultimate carrying capacity of section under short-time loading ($M = 0$; $\tau \to 0$).

P_u^∞ = ultimate carrying capacity of section under sustained loading ($M = 0$; $\tau \to \infty$).

e = eccentricity of column load.

e_{cr} = critical initial eccentricity of load P which causes creep failure after infinite time ($\tau \to \infty$).

e_u = eccentricity of load P which causes immediate static failure of column.

e'_u = eccentricity of load P which causes immediate static failure of column section.

e'_∞ = eccentricity of load P which causes failure of column section after infinite time.

h = distance between flanges in idealized column section.

l = length of column.

$n = \frac{E_s}{E_c}$; modular ratio.

t = time co-ordinate.

w = column deflection.

$\overline{w}$ = central column deflection.

$\overline{w}_0$ = initial central column deflection.

$\overline{w}_n$ = final central column deflection at time infinity.

$\alpha_1, \alpha_2, \alpha_3$ dimensionless parameters defining concrete strength and creep properties.

β_τ = stress causing failure in concrete when sustained for time interval τ.

β_0 = static concrete strength, $\tau \to 0$.

β_∞ = concrete strength under long sustained loading, $t \to \infty$.

$\delta = \frac{\overline{w}}{h}$; non dimensionalized column deflection.

δ_g = value of δ at which a change of phase occurs in the column.

$\delta_n = \frac{\overline{w}_n}{h}$.

$\delta_0 = \frac{\overline{w}_0}{h}$.

ϵ = strain.

ϵ_l = strain in left hand flange.

ϵ_{l0} = initial strain in left hand flange.

ϵ_r = strain in right hand flange.

ϵ_y = yield strain of steel reinforcement.

$\eta_c = \frac{4\pi^2 A_c E_c}{\lambda^2 P}$.

$\eta_s = \frac{4\pi^2 A_s E_s}{\lambda^2 P}$.

$\kappa = \frac{e}{h}$.

$\kappa_{cr} = \frac{e_{cr}}{h}$.

λ = slenderness ratio; for idealized section considered, $= \frac{2l}{h}$.

$\mu = \frac{A_s}{A_c}$.

$\zeta_1 = 1 + \frac{\beta_0}{\sigma_y}$.

$\zeta_2 = \frac{\beta_\infty + \mu\sigma_y}{\beta_0 + \mu\sigma_y}$.

σ = stress.

σ_l = concrete stress in left-hand flange.

σ_r = concrete stress in right-hand flange.

σ_{sl} = steel stress in left-hand flange.

σ_{sr} = steel stress in right-hand flange.

σ_y = yield stress of steel reinforcement.

τ = duration of load application.

$\Phi = \Phi_n(1 - e^{-\alpha_2 t})$; creep function.

Φ_g = value of Φ at which a change of phase occurs in the column.

Φ_n = value of Φ at time infinity.

Appendix — Sample Calculation; No. 15

The initial phase is I; the creep process involves the phase sequence I—II. Substitution of known values into Eqs. (4.1), (4.2) and (4.3) yields the following:

Phase I

$$\begin{aligned}
\delta_0 &= 0.238, \\
\epsilon_{l0} &= 0.00116\,(0.5 + 1.238\,\kappa), \\
\epsilon_l &= \epsilon_{l0}\, e^{-0.091\,\Phi} + 0.116\,(0.5 - 0.895\,\kappa)\,(1 - e^{0.091\,\Phi}) \\
&\quad + 0.0116\,\kappa\,[e^{0.126\,\Phi} - e^{-0.091\,\Phi}], \\
\frac{2\,\kappa + 1.056\,\delta}{2\,\kappa + 1.056\,\delta_0} &= e^{0.126\,\Phi}, \\
(\epsilon_r)_g &= 0.0017 - 0.01097\,\delta_g.
\end{aligned}$$

Phase II

$$\begin{aligned}
\delta &= C_1\, e^{0.2095\,\Phi} + C_2\, e^{-0{,}0575\,\Phi} + (0.3563 + \kappa), \\
\left(\frac{\partial\,\delta}{\partial\,\Phi}\right)_g &= \frac{1}{8.284}\,[86.20\,(\epsilon_r)_g + 2.10\,(\kappa + \delta_g) - 0.108].
\end{aligned}$$

A trial and error procedure is adopted to find the value of κ which satisfies the equation

$$\kappa = \kappa_{cr} = \frac{e'_u}{h} - \delta_n.$$

The value of $\frac{e'_u}{h}$ is found from Fig. 5 to be 0.500, hence

$$\kappa_{cr} + \delta_n = 0.5.$$

An initial value of $\kappa = 0.19$ is chosen, which yields the result

$$\kappa + \delta_n = 0.437.$$

From a second trial value, $\kappa = 0.25$,

$$\kappa + \delta_n = 0.571.$$

Interpolating, the third trial value, $\kappa = 0.22$, is obtained which provides the sufficiently accurate result

$$\kappa + \delta_n = 0.501.$$

The details of the three calculations are contained in Table 3.

Table 3. Sample Calculation

Trial	1	2	3
κ	0.190	0.250	0.220
δ_0	0.045	0.060	0.053
ϵ_{l0}	0.00085	0.00094	0.00090
$(\Phi)_g$	1.00	0.99	0.99
δ_g	0.100	0.123	0.115
$(\epsilon_r)_g$	0.0006	0.0004	0.0005
$\left(\frac{\partial \delta}{\partial \Phi}\right)_g$	0.0667	0.0863	0.0764
C_1	+0.125	+0.181	+0.151
C_2	−0.636	−0.740	−0.686
δ_n	0.247	0.321	0.281
$\delta_n + \kappa$	0.437	0.571	0.501

References

1. Kurt Gaede: «Knicken von Stahlbetonstäben unter Kurz- und Langzeitbelastung.» Deutscher Ausschuß für Stahlbeton, Heft 129; Berlin 1958.
2. Jose Nestor Distefano: "Creep Deflections in Concrete and Reinforced Concrete Columns." I.A.B.S.E. Publications, Vol. 21, 1961.
3. H. Rüsch: «Essai d'une nouvelle théorie de la flexion du béton armé.» Mémoires, centre d'études, de recherches et d'essais scientifiques du génie civil (C.E.R.E.S.) No. 2; Université de Liège, Décembre 1961.
4. S. A. Patel, B. Venkatraman: "Creep Behavior of Columns." PIBAL Report No. 422, Polytechnic Institute Brooklyn; May 1959.
5. E. Hognestad: "A Study of Combined Bending and Axial Load in Reinforced Concrete Members." Bulletin 399, Univ. of Illinois Eng. Exp. Stn., November 1951.

6. R. F. WARNER, C. L. HULSBOS: "Probable Fatigue Life of Prestressed Concrete Flexural Members." Fritz Laboratory Report No. 223.24A; Lehigh University; July 1962.
7. F. DISCHINGER: «Untersuchungen über die Knicksicherheit, die elastische Verformung und das Kriechen des Betons bei Bogenbrücken.» Bauingenieur, Vol. 20, 1939. Also Vol. 18, 1937.

Summary

In an introductory study of creep failure in reinforced-concrete columns, the case of a pin-ended member subjected to an eccentrically applied sustained thrust P is considered. A critical initial eccentricity e_{cr} is defined for which the time of loading required to cause failure, τ, is equal to infinity. If the eccentricity of the load P is greater than e_{cr}, creep effects cause column failure after a finite time interval (Finite Life Problem); if however the initial eccentricity is not greater than e_{cr}, creep effects increase the column deflection, but never to a sufficient extent to cause failure.

A theoretical analysis is made of the creep behavior of a reinforced concrete column of idealized I section. Equations are obtained which allow the initial critical eccentricity e_{cr} to be determined by a trial and error procedure. Although simplified strength, stress-strain and creep relations are used to represent the concrete properties, the analysis indicates essential column behavior and the prime variables of the problem. A numerical example shows the considerable decrease in column load carrying capacity brought about by concrete creep.

Résumé

Dans cette étude préliminaire, les auteurs examinent l'influence du fluage sur la rupture des colonnes en béton armé. Ils examinent d'abord le cas d'une colonne rectiligne bi-articulée, soumise à un effort excentré permanent P. L'excentricité initiale critique pour laquelle la rupture se produit au bout d'un temps infini est désignée par e_{cr}. Si l'excentricité initiale de la charge dépasse la valeur e_{cr}, le fluage du béton entraîne la rupture de la colonne au bout d'un temps fini. Si l'excentricité est inférieure à e_{cr}, le fluage du béton entraîne bien une augmentation de la flèche, mais dans une mesure trop faible pour entraîner la rupture.

Pour une colonne en béton armé de section en double-té idéalisé, les auteurs établissent des équations permettant de déterminer l'excentricité initiale critique e_{cr} par la méthode des approximations successives. Bien que les propriétés du béton telles que la résistance, le diagramme contrainte-déformation et le fluage soient représentées par des relations simplifiées, l'étude fait ressortir les principaux paramètres intervenant sur le comportement dans le temps de colonnes en béton armé. Un exemple numérique montre la réduction considérable de la résistance d'une colonne du fait du fluage du béton.

Zusammenfassung

Die vorliegende Arbeit untersucht den Einfluß des Betonkriechens auf das Versagen von Stahlbetonsäulen. Der Fall eines ursprünglich geraden und beidseitig gelenkig gelagerten Stabes unter einer konstanten exzentrischen Last P wird untersucht. Die kritische Exzentrizität, für die Versagen nach unendlicher Zeit, $\tau \to \infty$, eintritt, wird als e_{cr} definiert. Überschreitet die tatsächliche Anfangsexzentrizität der Last den Wert e_{cr}, so erreicht der Stab den Bruchzustand in der endlichen Zeit τ. Ist aber die Exzentrizität kleiner als e_{cr}, dann wächst zwar die Ausbiegung infolge des Betonkriechens, ohne jedoch zum Bruch zu führen.

Für eine Stahlbetonsäule mit idealem I-Querschnitt werden Beziehungen hergeleitet, die eine iterative Bestimmung von e_{cr} ermöglichen. Obgleich die Betoneigenschaften durch vereinfachte Festigkeit-, Spannung-Dehnung- und Kriechen-Beziehungen erfaßt werden, zeigt die Untersuchung die Hauptparameter für das zeitabhängige Verhalten einer Stahlbetonsäule. Numerische Beispiele zeigen die beträchtliche, vom Betonkriechen verursachte Verminderung des Stabwiderstandes.